

1 Supporting Information

2

3

4 Engineering FeNi Alloy Nanoparticles *via* Synergistic Ultralow Pt Doping and
5 Nanocarbon Capsulation for Efficient Hydrogen Evolution

6 Aixin Fan, Congli Qin, Xin Zhang,* Juntao Yang, Jiaqi Ge, Shiqing Wang, Xiaolin Yuan, Su Wang and
7 Xiaoping Dai

8

9 State Key Laboratory of Heavy Oil Processing, College of Chemical Engineering, China University of
10 Petroleum, Beijing, 102249, China

11 *Corresponding author. Xin Zhang*

12 E-mail: zhangxin@cup.edu.cn

14 **Experimental section:**

15 **1. Characterization**

16 Power X-ray diffraction (XRD) was tested on a Brüker D8 Advance diffractometer at 40 kV and 40 mA
17 for Cu K α ($\lambda = 0.15406$). Scanning electron microscope (SEM) images were observed on an ULTRA 55 SEM
18 at 20 kV. Transmission electron microscopy (TEM) was performed on JEM-2100 at 200 kV. High-resolution
19 transmission electron microscopy (HRTEM) was performed on a Tecnai G² F20 S-Twin at 200 kV. High-
20 angle annular dark field scanning transmission electron microscopy (HAADF-STEM) was carried out on
21 Tecnai G² F20 S-Twin HRTEM operating at 200 kV. X-ray photoelectron spectra (XPS) was measured on a
22 PHI 5000 Versaprobe system using monochromatic Al K α radiation (1486.6 eV). The C 1s graphitic peak
23 (284.6 eV) is referred to as the reference. Inductively coupled plasma optical emission spectrometer (ICP-
24 OES) was performed on iCAP7400 (Thermo Fisher Scientific). Renishaw Micro-Raman System 2000
25 spectrometer with spectral resolution of 2 cm⁻¹ was used to record Raman spectra. A laser line at 532 nm of a
26 He/Cd laser was used as an exciting source, and the output power was 20 mW. The spectra were recorded at
27 a 1 cm⁻¹ resolution with the condition of 50 s integral time at room temperature. N₂ adsorption/desorption
28 isotherms were conducted at -196 °C using a kubo X10000 static volumetric gas adsorption instrument. The
29 samples were degassed at 200 °C for 3 h in a vacuum before measurements. The specific surface area of the
30 sample was calculated from the adsorption branches (p/p_0 : 0.05–0.20) by the Brunauer–Emmett–Teller (BET)
31 method. The mesopore size distribution was calculated from desorption branches by the
32 Barret–Joyner–Halenda (BJH) method, and the single point adsorption total pore volume was taken at the
33 relative pressure of 0.96.

34 **2. Calculation method**

35 Electrochemically active surface area (ECSA) was estimated from the double-layer capacitance (C_{dl})
36 measurements. The C_{dl} was obtainbed from a series of CVs measured from the potential range of 0.52 to 0.62
37 V (vs RHE).

38 The mass activity and turnover frequency (TOF) of the catalysts were calculated according to the
39 following equations

40 mass activity = j / m (1)

41 $TOF = J \times A / (2 \times F \times n)$ (2)

42 where J is taken from the current density at a specific overpotential (mA cm^{-2}), A is 0.07065 cm^2 (the
43 geometric area of GC), F is $96\,485 \text{ mol C}^{-1}$ (the Faraday constant), and n is the number of total moles of Pt.

44 Faradic efficiency of the HER was calculated by the ratio of the H_2 produced in cathode to the theoretical
45 amount of H_2 . The generated H_2 was collected by a water drainage method and then the molar of H_2 was
46 obtained using the ideal gas law. The corresponding theoretical H_2 value was determined by assuming that
47 HER was the only process that took place in cathode (100% electrolysis efficiency).^{1,2}

48 Table S1. Compositions of FeNi@C, Pt-FeNi@C and Pt-FeNi@C-0.19 wt% determined by ICP-OES and
49 EDAX.

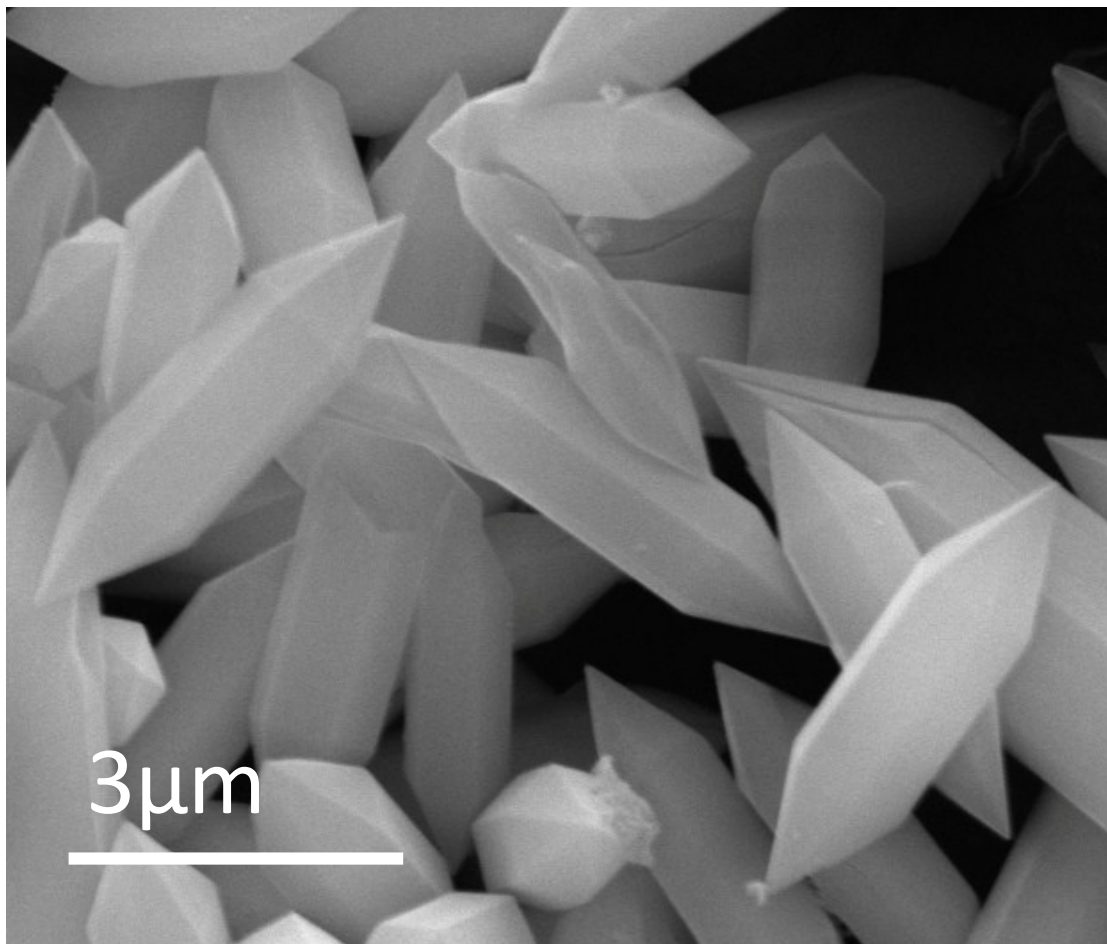
50

Sample	Bulk content (wt%) by ICP-OES			
	Pt	Ni	Fe	Ni:Fe (atom)
FeNi@C	-	17.60	37.00	1:2.10
Pt-FeNi@C	0.66	16.96	35.47	1:2.09
Pt-FeNi@C-0.19 wt%	0.19	17.08	36.80	1:2.15

51

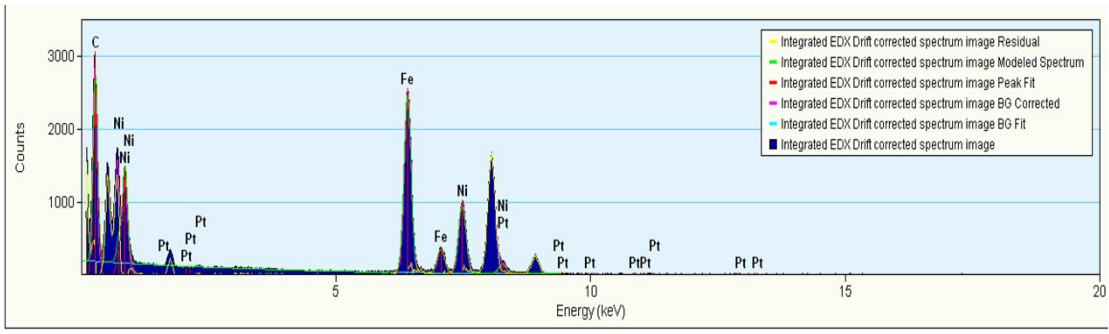
Sample	Surface content (wt%) by EDAX			
	Pt	Ni	Fe	Ni:Fe (atom)
FeNi@C	-	13.44	29.14	1:2.27
Pt-FeNi@C	0.04	12.96	29.80	1:2.41
Pt-FeNi@C-0.19 wt%	-	13.25	29.27	1:2.32

53

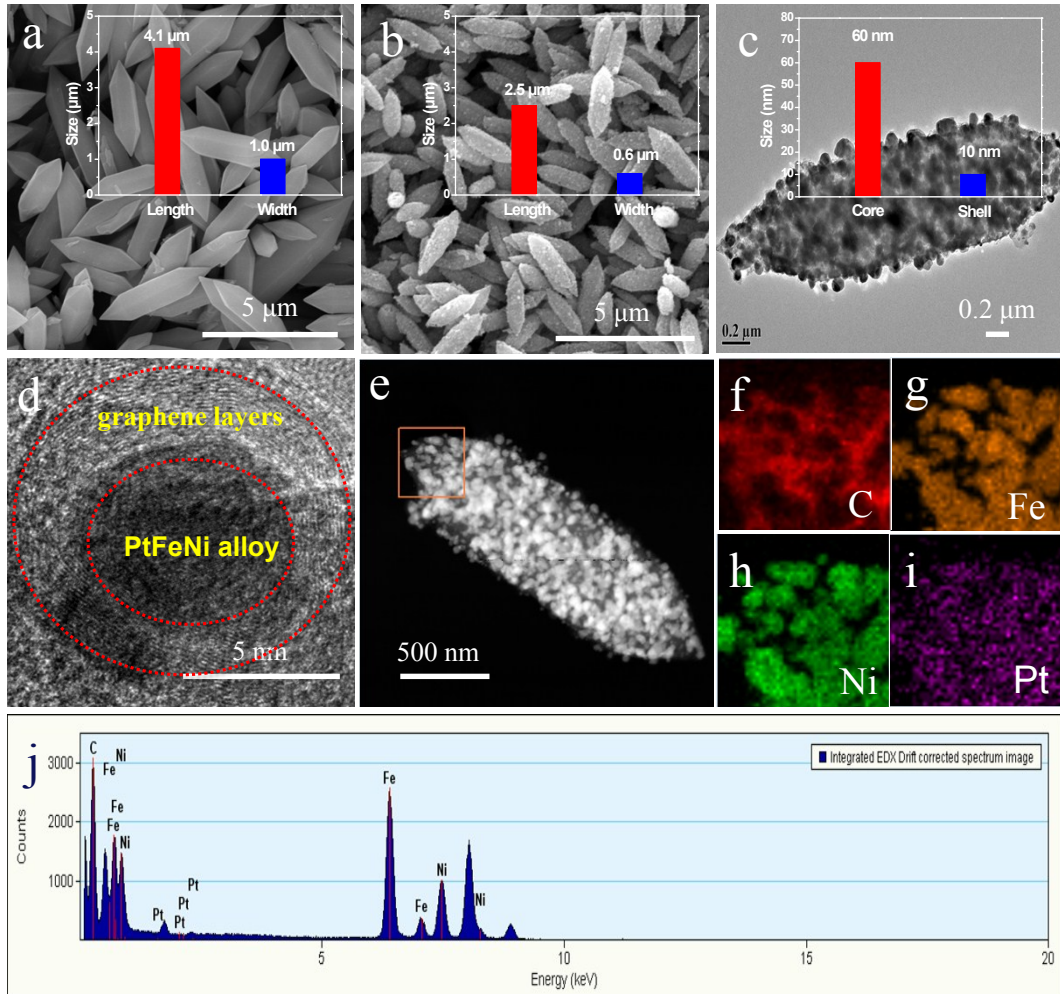


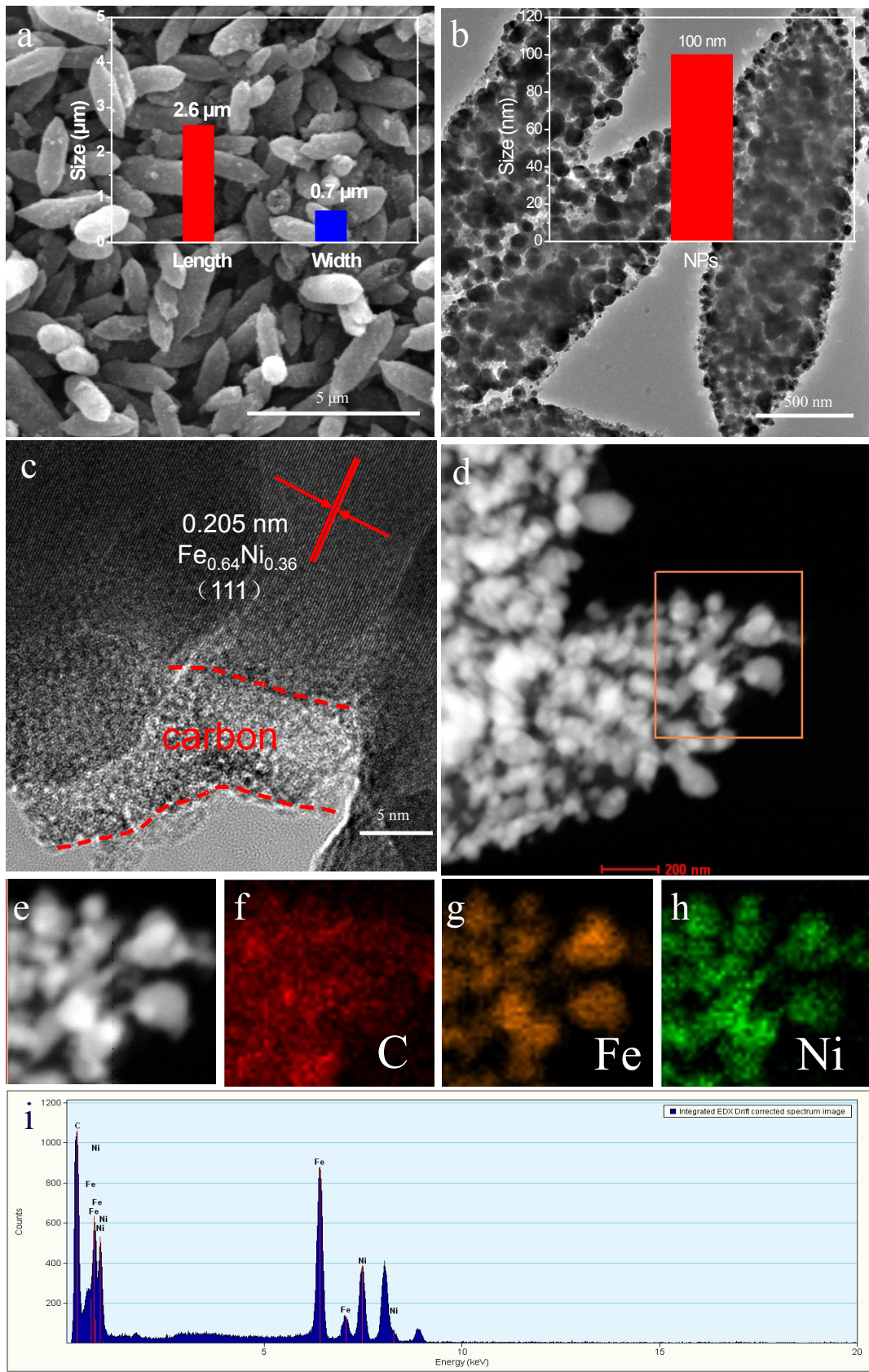
54

55 Figure S1. SEM image of FeNi-MOF.



58 **Figure S2.** EDX analysis of the Pt-FeNi@C.

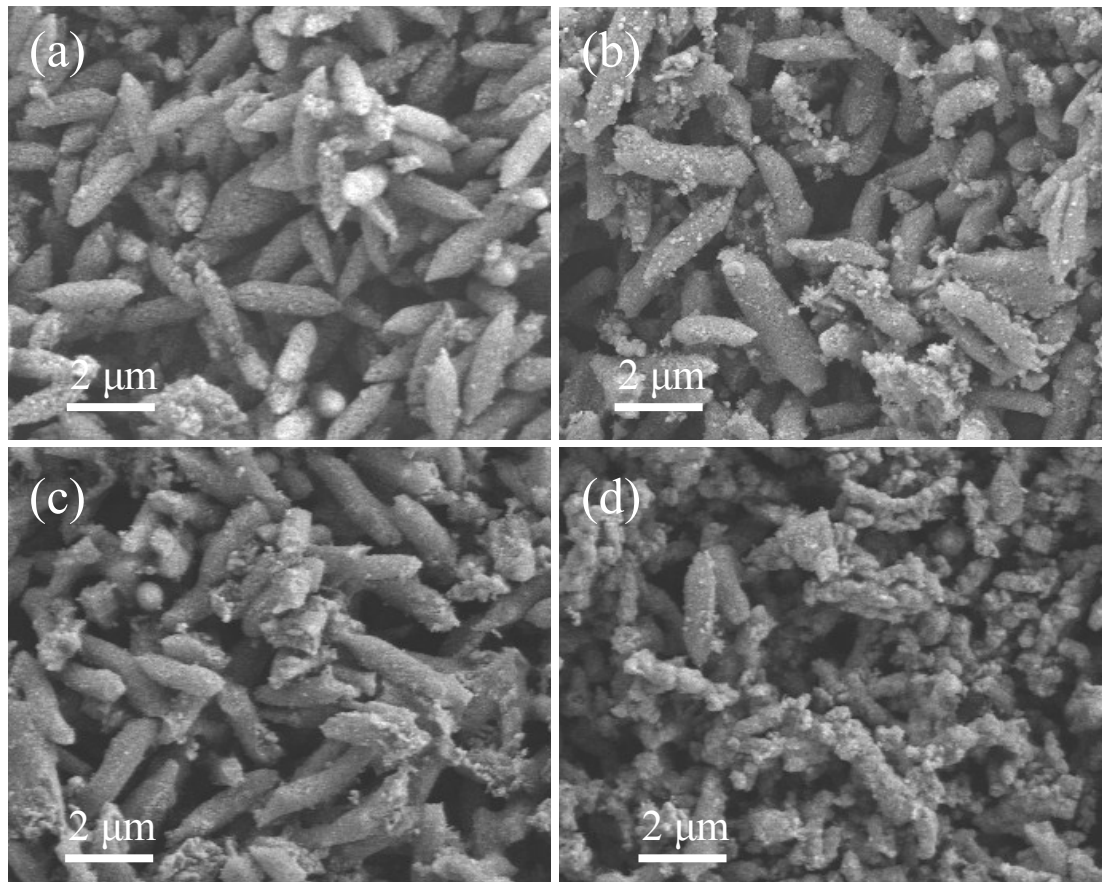




65

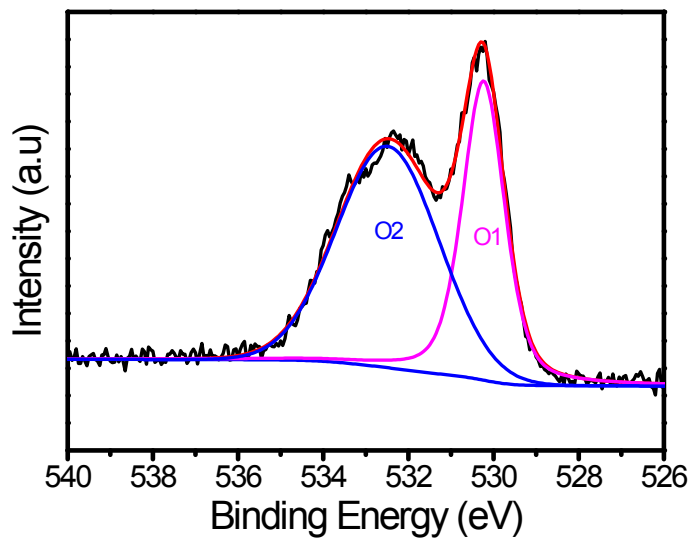
66 **Figure S4.** (a) SEM, (b) TEM, and (c) HRTEM images of $\text{FeNi}@\text{C}$ (inset: size distribution histogram). (d-h)

67 HAADF-STEM image and corresponding EDX mapping of $\text{FeNi}@\text{C}$. (i) EDX analysis of the $\text{FeNi}@\text{C}$.



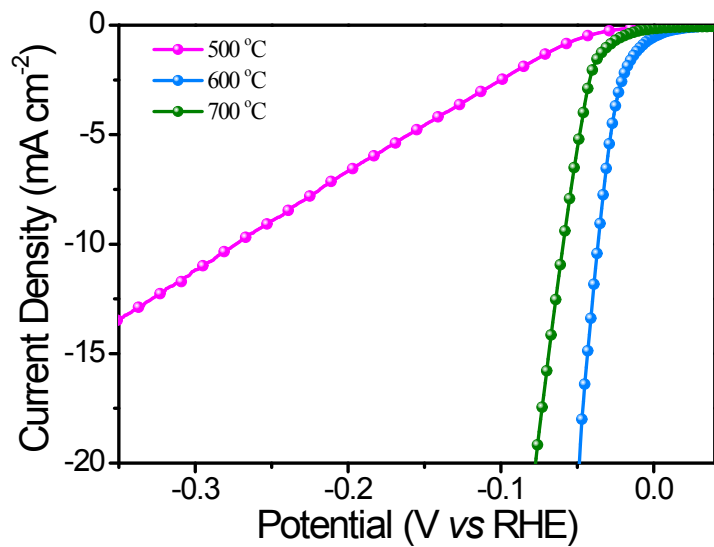
68

69 **Figure S5.** SEM images of Ru-FeNi@C, Au-FeNi@C, Pd-FeNi@C and Ag-FeNi@C samples.



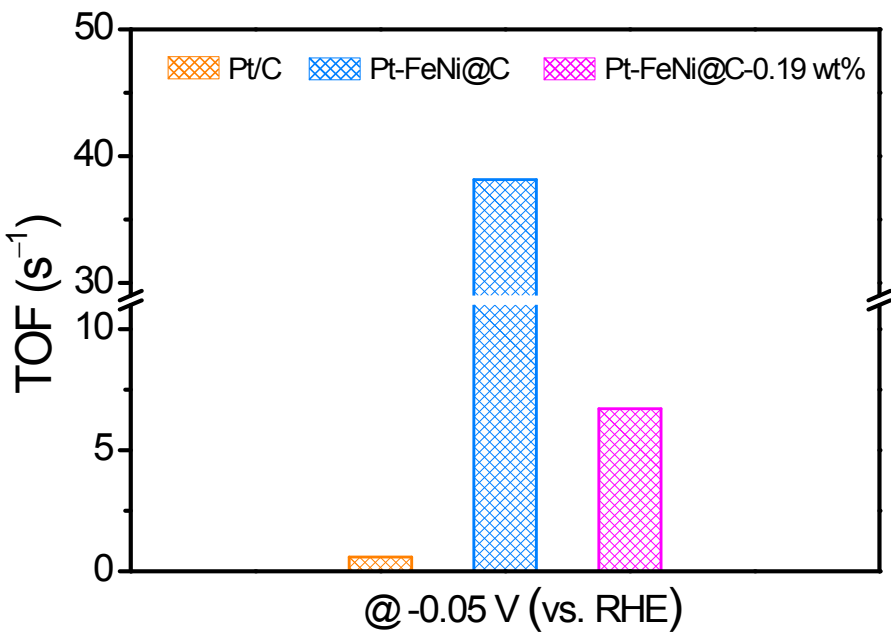
71

72 **Figure S6.** The high resolution XPS spectra for O 1s of Pt-FeNi@C. The peak O1 corresponds to metal–
73 oxygen bonds while the peak O2 could be attributed to oxygen in –OH groups.³



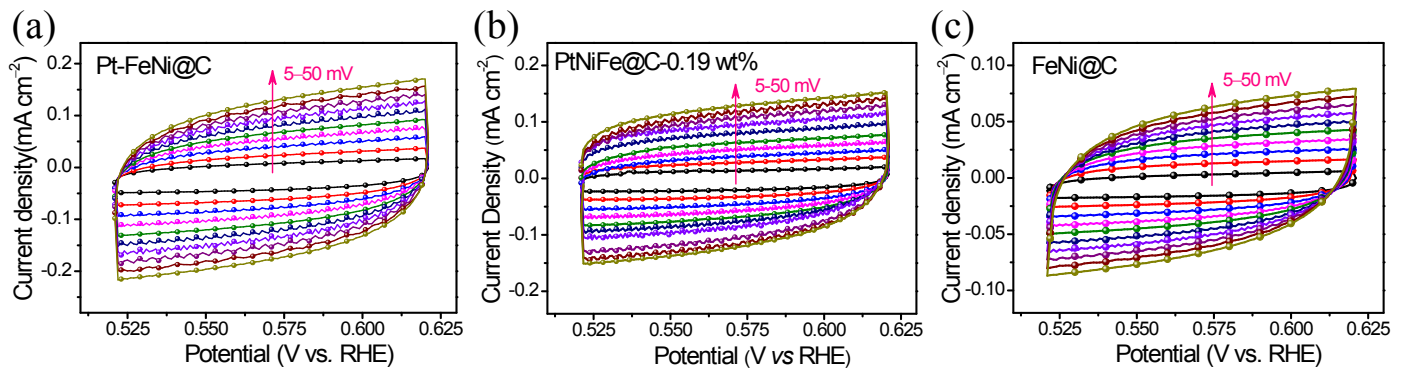
75

76 **Figure S7.** LSV polarization curves of catalysts with different annealing temperature.



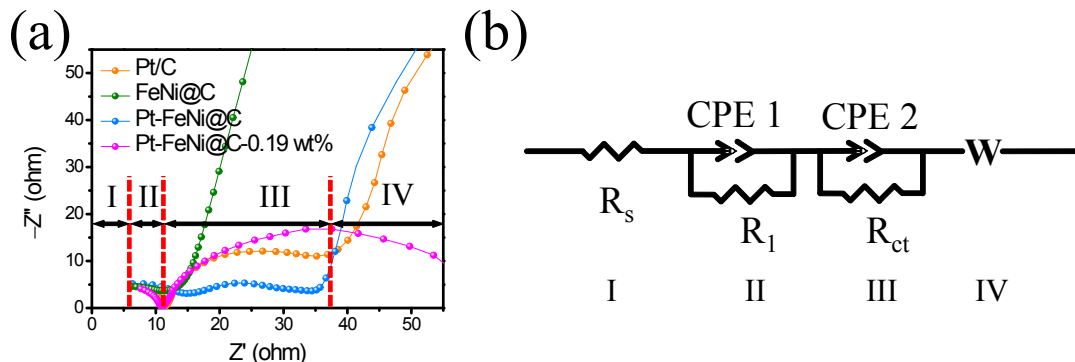
78

79 **Figure S8.** TOF values at the overpotential of 50 mV.



81

82 **Figure S9.** CV curves at different scan rates for (a) Pt-FeNi@C, (b) Pt-FeNi@C-0.19 wt% and (c) FeNi@C.



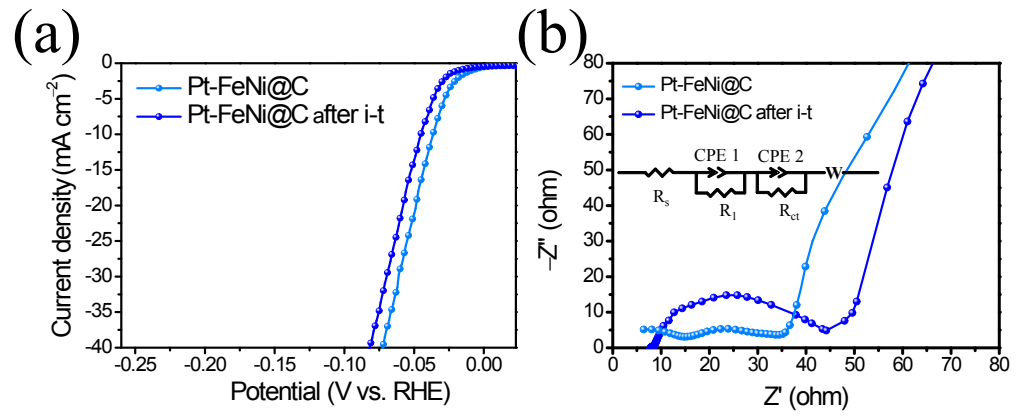
84

85 **Figure S10.** (a) Electrochemical impedance spectra (EIS) of commercial Pt/C, FeNi@C, Pt-FeNi@C, and Pt-
86 FeNi@C-0.19 wt% catalysts; (b) electric equivalent circuit model was used to fit EIS procedures.

87 **Table S2.** Summary of R_s and R_{ct} for different samples by fitting the Nyquist plots using the equivalent
88 circuit model.

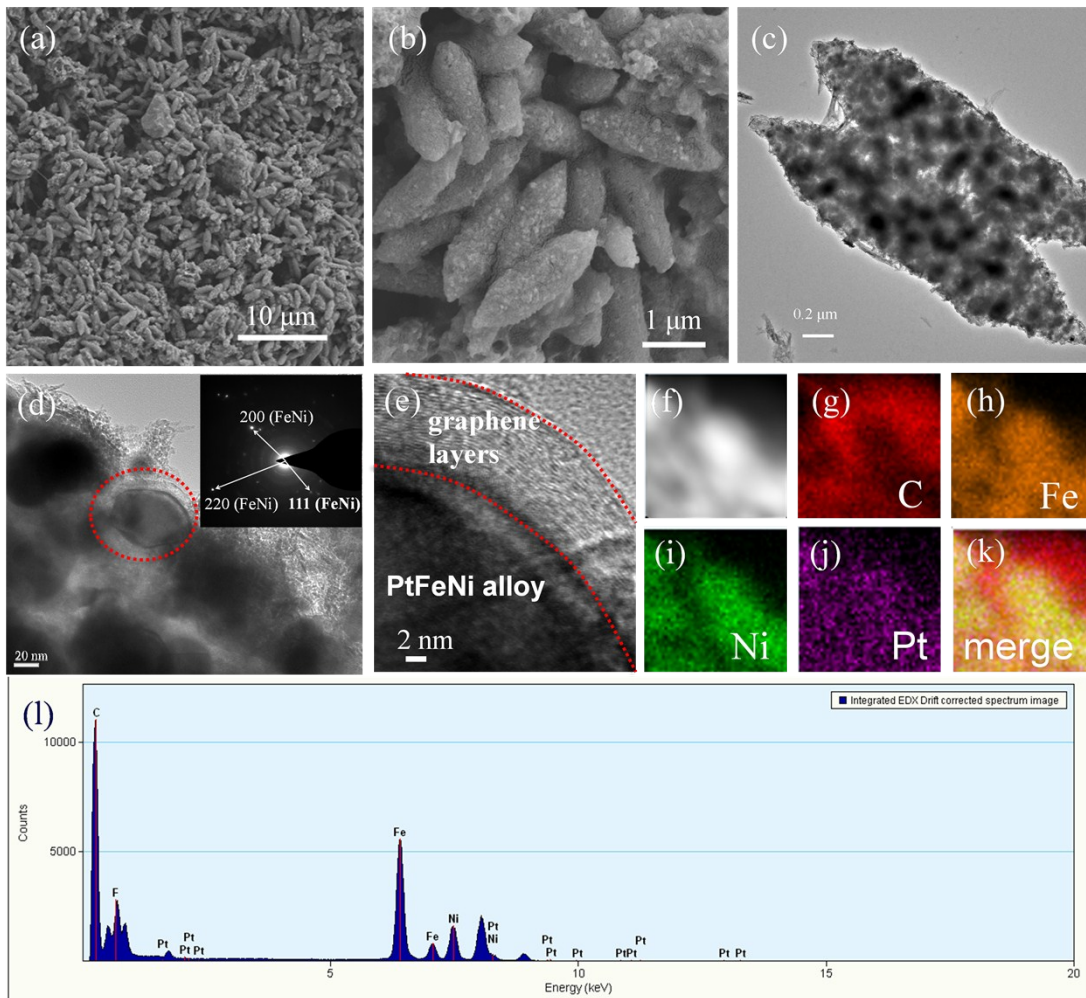
Samples	R_s (Ohm)	R_{ct} (Ohm)
Pt-FeNi@C	6.19	19.91
Pt/C	7.92	28.56
Pt-FeNi@C-0.19 wt%	7.69	47.97
FeNi@C	6.25	9218

89



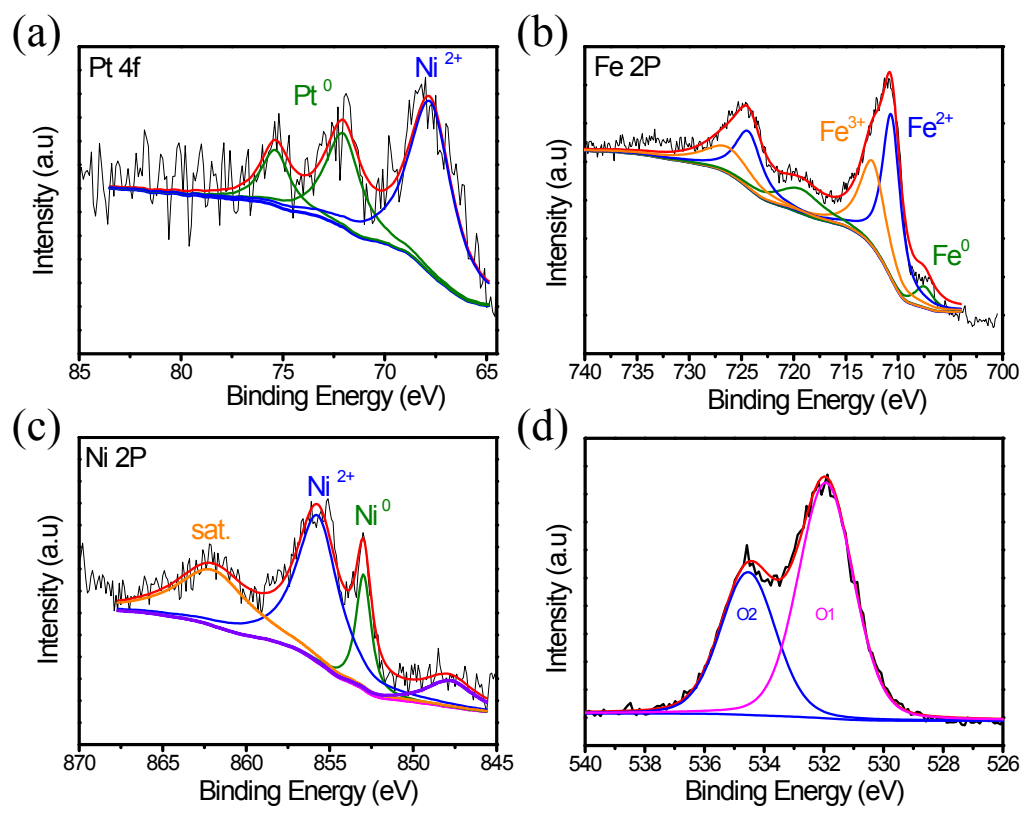
91

92 **Figure S11.** (a) EIS and LSV analyses of Pt-FeNi@C before and after *i-t* test.



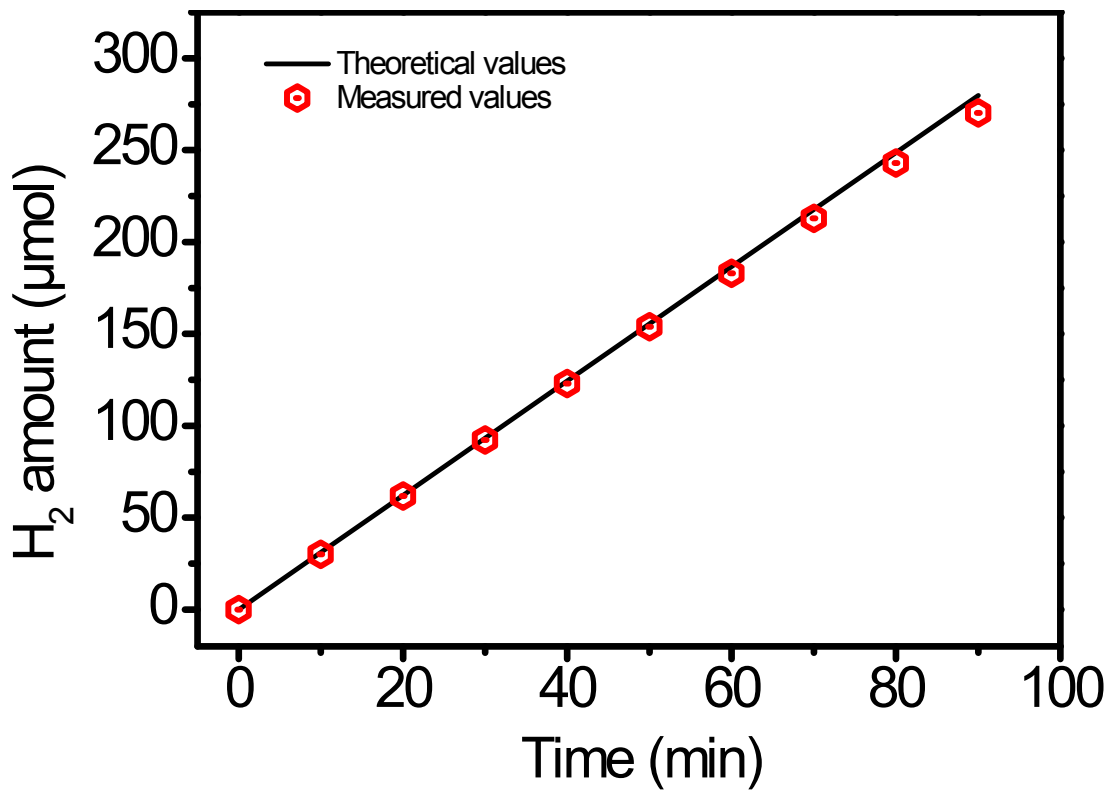
95 **Figure S12.** (a-l) The SEM, TEM, SAED pattern, HR-TEM, STEM and EDX analyses of post electrocatalyst

96 for Pt-FeNi@C. (The F element could be correlated to Nafion.)



98

99 **Figure S13.** (a-d) XPS analyses of post electrocatalyst for Pt-FeNi@C.



101

102 **Figure S14.** Faradaic efficiency of Pt-FeNi@C for HER.

103

105 Table S3. Comparison of the electrocatalytic HER properties of the high performance electrode materials
 106 reported in recent literatures.

107

Catalysts	Electrolyte	Specific activity / η (mA cm ² / mV)	Content of Pt wt%	References
Pt-FeNi@C	0.5 M H ₂ SO ₄	21/50	0.16	This work
ALD50Pt/NGNs	0.5 M H ₂ SO ₄	15/50	2.1	4
Pt _{1.8} MoS ₂	0.5 M H ₂ SO ₄	2/50	—	5
MoS ₂ @Pt-3	0.5 M H ₂ SO ₄	5/50	0.41	6
Pt-MoO ₂ /MWCNTs	0.5 M H ₂ SO ₄	10/50	0.5	7
Pt ₂₃ Ni ₇₇ /C	0.5 M H ₂ SO ₄	58/50	72.2	8
DR-MoS ₂ -Pt	0.5 M H ₂ SO ₄	30/50	—	9
Pt Sas/DG	0.5 M H ₂ SO ₄	53/50	2.1	10
CDs/Pt-PANI-4	0.5 M H ₂ SO ₄	35/50	—	11
Pt/CNTs-ECR	0.5 M H ₂ SO ₄	25/50	0.2	12
Ru-NGC	0.5 M H ₂ SO ₄	40/50	6.55	13

109 **References:**

- 110 1 Y. Liu, Q. Li, R. Si, G. Li, W. Li, D. Liu, D. Wang, L. Sun, Y. Zhang and X. Zou, *Adv. Mater.*, 2017,
- 111 29, 1606200.
- 112 2 C. Zhong, Q. Zhou, S. Li, L. Cao, J. Li, Z. Shen, H. Ma, J. Liu, M. Lu and H. Zhang, *J. Mater. Chem.*
- 113 A, 2019, 7, 2344–2350.
- 114 3 P. W. Menezes, C. Panda, S. Garai, C. Walter, A. Guiet and M. Driess, *Angew. Chem., Int. Ed.*,
- 115 2018, 57, 15237–15242.
- 116 4 N. Cheng, S. Stambula, D. Wang, M. N. Banis, J. Liu, A. Riese, B. Xiao, R. Li, T. K. Sham, L. M. Liu,
- 117 G. A. Botton and X. Sun, *Nat. Commun.*, 2016, 7, 1–9.
- 118 5 X. Chia, N. A. A. Sutrisnoh and M. Pumera, *ACS Appl. Mater. Interfaces*, 2018, 10, 8702–8711.
- 119 6 X. Y. Xu, X. F. Dong, Z. J. Bao, R. Wang, J. G. Hu and H. B. Zeng, *J. Mater. Chem. A*, 2017, 5,
- 120 22654–22661.
- 121 7 X. Xie, Y. F. Jiang, C. Z. Yuan, N. Jiang, S. J. Zhao, L. Jia and A. W. Xu, *J. Phys. Chem. C*, 2017,
- 122 121, 24979–24986.
- 123 8 S. Wang, G. Yang and S. Yang, *J. Phys. Chem. C*, 2015, 119, 27938–27945.
- 124 9 J. Xie, L. Gao, H. Jiang, X. Zhang, F. Lei, P. Hao, B. Tang and Y. Xie, *Cryst. Growth Des.*, 2019, 19,
- 125 60–65.
- 126 10 Y. Qu, B. Chen, Z. Li, X. Duan, L. Wang, Y. Lin, T. Yuan, F. Zhou, Y. Hu and Z. Yang, *J. Am. Chem.*
- 127 *Soc.*, 2019, 141, 4505–4509.
- 128 11 Q. Dang, Y. Sun, X. Wang, W. Zhu, Y. Chen, F. Liao, H. Huang and M. Shao, *Appl. Catal. B Environ.*,
- 129 2019, 257, 117905.
- 130 12 X. Bao, Y. Gong, Y. Chen, H. Zhang, Z. Wang, S. Mao, L. Xie, Z. Jiang and Y. Wang, *J. Mater.*

131 *Chem. A*, 2019, **7**, 15364–15370.

132 13 Q. Song, X. Qiao, L. Liu, Z. Xue, C. Huang and T. Wang, *Chem. Commun.*, 2019, **55**, 965–968.

133